DesignCon 2019

On the Minimization of PCB Differential Pair Skew
Or
Its Effect

Syed. A. Bokhari, Fidus Systems Inc.

Syed.Bokhari@fidus.com

Abstract

This paper presents two new methods for dealing with skew in Printed Circuit Board (PCB) differential pairs. In the first method, skew arising from fiber-weave effect is minimized by using a non-uniform differential pair.   It consists of a hybrid combination of edge-coupled and broadside-coupled differential geometries. Further, the P- and N-traces are routed as "complementary twisted pairs" so that both traces see nearly the same environment. Simulations using a three dimensional electromagnetic field solver shows a significant reduction in fiber weave Skew.

Differential insertion loss is strongly affected by skew which can result in complete fading at a precise frequency and its integral multiples. When this frequency approaches the fundamental frequency of data, eye opening reduces leading to an increased Bit Error rate (BER). If this undesirable effect of skew can be reduced, it will become possible to operate at high data rates even in the presence of substantial skew. In this work, it is discovered that it is possible to reduce the effect of skew by the use of strongly coupled differential elements. Two or more of these elements need to be inserted at certain locations along the link path. They result in a significantly reduced fading. An exact analytical solution is derived for the differential insertion loss of an interconnect link comprising two tightly coupled sections. Numerical results illustrate the performance improvement achievable.

Author Biography

Syed. A. Bokhari   received the BE degree in Electronics Engineering from the Visveswaraya College of Engineering of Bangalore University in 1980, The M.Sc.(Eng.) degree in Electrical Communication Engineering from the Indian Institute of Science (IISc), Bangalore, India in 1982 and the Ph.D. degree from the Department of Aerospace Engineering, IISc in 1986. He is currently a Technical Manager of Signal Integrity and EMC at Fidus Systems Inc., Ottawa, Canada. Prior to this, he has held positions of Senior Member of Consulting Staff at Cadence Design Systems (Canada) Ltd., Senior Research Associate at the Department of Electrical Engineering, University of Ottawa, Research Associate at the Laboratory of Electromagnetism and Acoustics of the Swiss Federal Institute of Technology in Lausanne, Switzerland, and Senior Research Fellow at IISc. He was the Technical Papers Co-Chair of the 2016 IEEE EMC Symposium in Ottawa and the co-editor of the IEEE Transactions on EMC conference special issue. He is currently the chairman of the IEEE Ottawa EMC Chapter.

He is the recipient of the outstanding paper award at EDICON 2017. His areas of research interests include Printed Circuit Board design for Signal and Power Integrity and EMC, Numerical Methods in Electromagnetics, and Miniaturized Antennas. He has published extensively in these areas and holds two patents.

1. Introduction

When a serial link design satisfies certain requirements on its s-parameters and channel operating margin [1], error free data transmission is generally assured with high confidence. Differential-Insertion loss (IL), Return loss (RL), Insertion loss Deviation (ILD), and Insertion loss to cross talk ratio (ICR) or Integrated Crosstalk Noise (ICN) are the primary parameters that determine link performance (Figure 1). All of these are affected by the skew in the differential pair comprising a P- and an N-interconnect.

Skew in a differential pair can result from a number of sources [2]. Any asymmetry in the routing of the P- and N-traces will lead to skew. Some of the sources are summarized in Table 1. They can be deterministic in most cases, or random due to manufacturing tolerances. Most copper features can result in values of skew up to ~1 picosecond. Physical pin length difference in connectors can result in larger values of skew. The effect of all deterministic sources can be reduced using well known procedures. Sources that are random in nature can also be dealt with through tighter manufacturing tolerances. One source of skew in all fiber/resin composite printed circuit boards is due to their inhomogeneity and anisotropy.
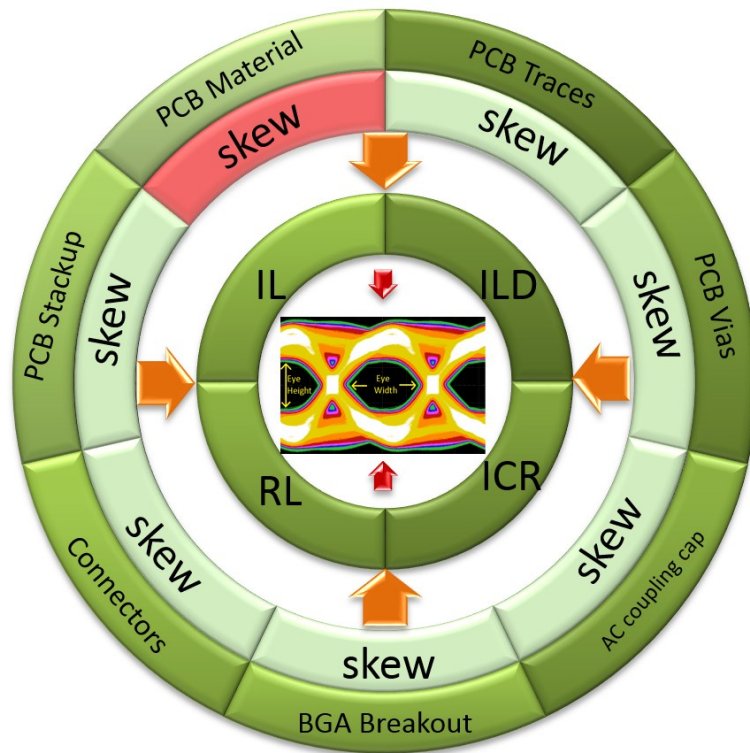

Figure 1: Illustration of SERDES Eye opening dependence

Fiber weave induced skew in a differential pair can be the most dominant mechanism and is the primary reason for pair-to-pair and board to board variations [3]. This subject has been well researched both theoretically as well as experimentally and many solutions exist [4-11].

#	Source of Skew	~ Value (pS)
1	Backdrill tolerance, Tear Drop asymmetry, Trace bends, GND via asymmetry	1
2	Connector pin length	5
3	Glass Fiber Weave	5+

Table 1: Skew sources and their approximate impact

Note that "skew" itself is not listed as a fundamental parameter of importance. It is its effect on the differential s-parameters that is important. First, skew results in common mode signal generation. In a multi-board system with inadequate "ground integrity", these high frequency common mode signals can excite resonances in the ground structure. This will eventually lead to an increased ILD and ICR. Secondly, skew results in fading at a precise frequency and its integral multiples. If this frequency is less than or close to the Nyquist frequency, bits in the data pattern that have substantial harmonic content at this frequency will not be received and the Bit Error Rate (BER) will increase.

In this work, we first present a new transmission line configuration for the reduction of fiber weave skew. By recognizing that this is primarily due to a periodic non-uniformity in the dielectric constant of the substrate material, a new non-uniform transmission line geometry that counters this effect is proposed. This type of transmission line has some interesting frequency dependent characteristics that can be exploited in creating tightly coupled lines. Secondly, it is observed that cascading multiple sections of tightly coupled lines is beneficial in reducing the null in the insertion loss. Numerical results are illustrated using Ansys HFSS and Keysight ADS.

2. A non-Uniform interconnect

Uniform edge coupled differential transmission lines are the most commonly used forms of PCB interconnect. It can be very difficult or even impossible to maintain uniformity in a real PCB. Routing in BGA and connector pin fields is inevitable and these present a non-uniform environment. Further, the PCB substrate itself presents a non-uniform environment in most cases. Interestingly, this non-uniformity tends to be periodic in nature. By introducing an intentional periodic non-uniformity in a uniform interconnect, one is able to correct for undesirable effects arising from the environment. This has been used earlier to reduce impedance variations and cross talk [12]. By a suitable modification, it can be designed to ensure that each P or N trace of a differential pair perceives the same environment.

A broadside coupled differential pair geometry is known to require thicker dielectric substrates. The edge-coupled differential pair has a primary advantage that it can be implemented with a reduced PCB thickness and layer count as shown in Figure 2. The broadside coupled trace geometry can be modified by offsetting the two traces as shown. This reduces the coupling between traces and also reduces the layer thickness required for a given impedance. While there is no apparent advantage in this configuration, it helps in the construction of a pseudo- twisted pair.

To estimate the improvement in skew reduction feasible, we first consider the case of a straight broad-edge differential pair as shown in Figure 3. The substrate has three single ply 1080 style weaves stacked with their weave patterns perfectly aligned to result in a maximum lateral variation in the dielectric constant. The geometry has W = 4 mils, S = 10 mils, D1=D3 = 4 mils, D2 = 3 mils, and T = 0.6 mil. A dielectric constant value of 6 and loss tangent = 0.02 is assumed for the glass bundles. A dielectric constant value of 2 and loss tangent = 0.01 is assumed for the resin. The length of the transmission line is assumed to be 200 mils. 3D EM simulations were carried out using Ansys' HFSS. Computed s-parameters are shown in Figure 3. Skew in time domain as obtained from the phase difference of the single ended insertion loss is 18 pS/inch. It can also be seen that this differential pair has very low Far End Cross Talk (FEXT) between its P and N traces.

The non-uniform interconnect is constructed by sweeping a rectangle (trace cross-section) along a curve defined by the equation

$$x(t) = t, and \ y(t) = \left(\frac{S+W}{2}\right)\left(Cos\left(\frac{\pi t}{10}\right) - 1\right), 0 \ \leq t \ \leq \ 200 \ mils \qquad (1)$$

The N-Trace on a different layer is a mirror image of the P-trace as shown in Figure 4. All other physical parameters are the same as the geometry of Figure 3. Computed skew in this case is less than 0.03pS/inch. An important observation here is that the FEXT value increases substantially with frequency.

It is easy to see that by controlling the periodicity of the line, the number of overlapping twists can be made to vary. Increasing the number of twists per inch will decrease the P-N skew and will also increase the cross talk between the two lines.
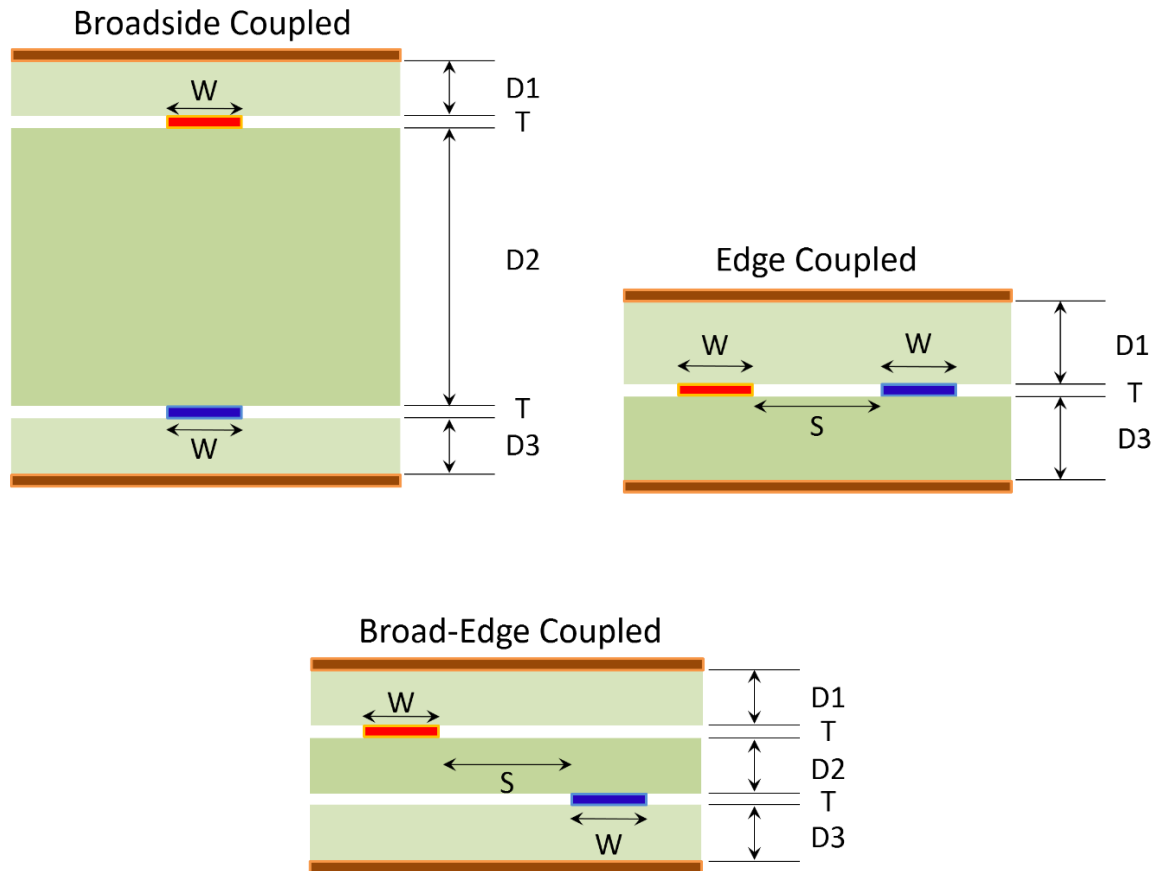
Coupling Type	W	T	D1	D2	D3	Z_s	Z_m	$Z_{diff} = 2 (Z_s - Z_m)$
Broadside	4	0.6	3	15	3	54	4	100
Edge	4	0.6	4.5	-	4.5	52	2	100
Broad-Edge	4	0.6	3.4	3	3.4	52	2	100

Figure 2: Differential transmission line geometries (All dimensions are in mils to scale)
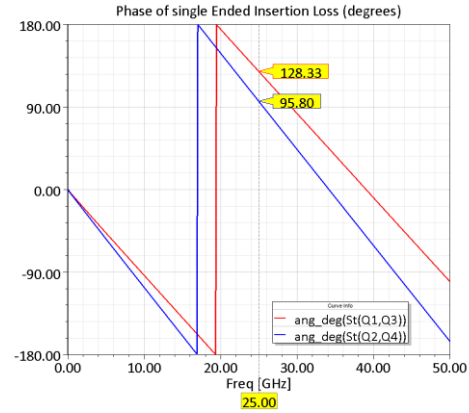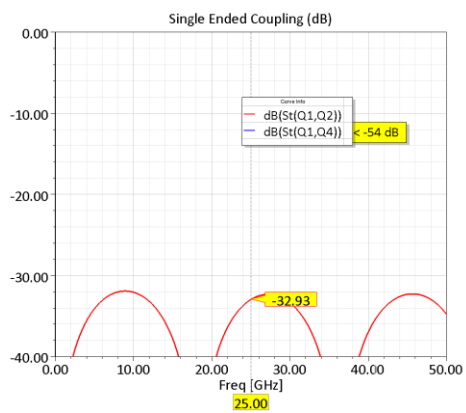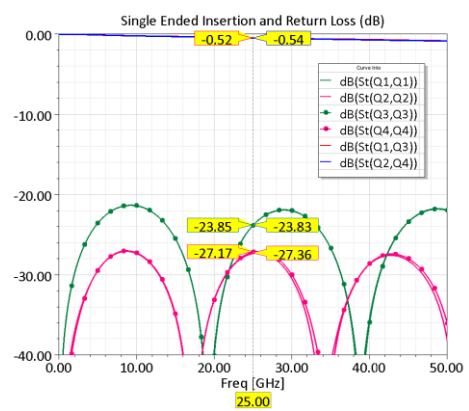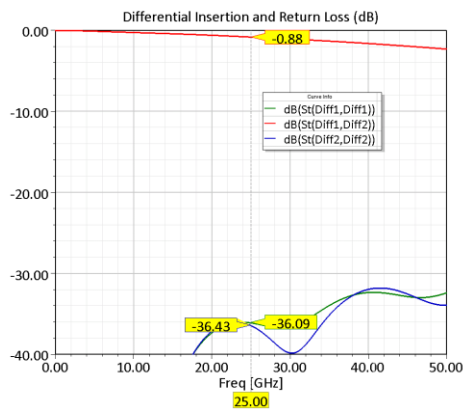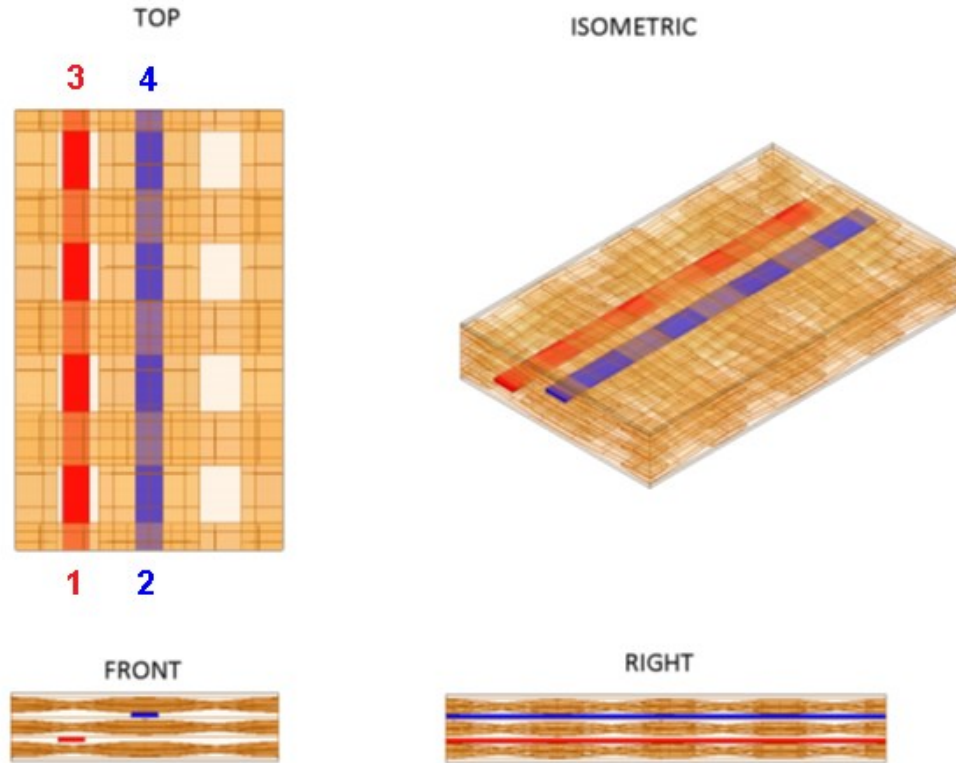
Figure 3: Reference straight 200 mils long broad-edge line geometry
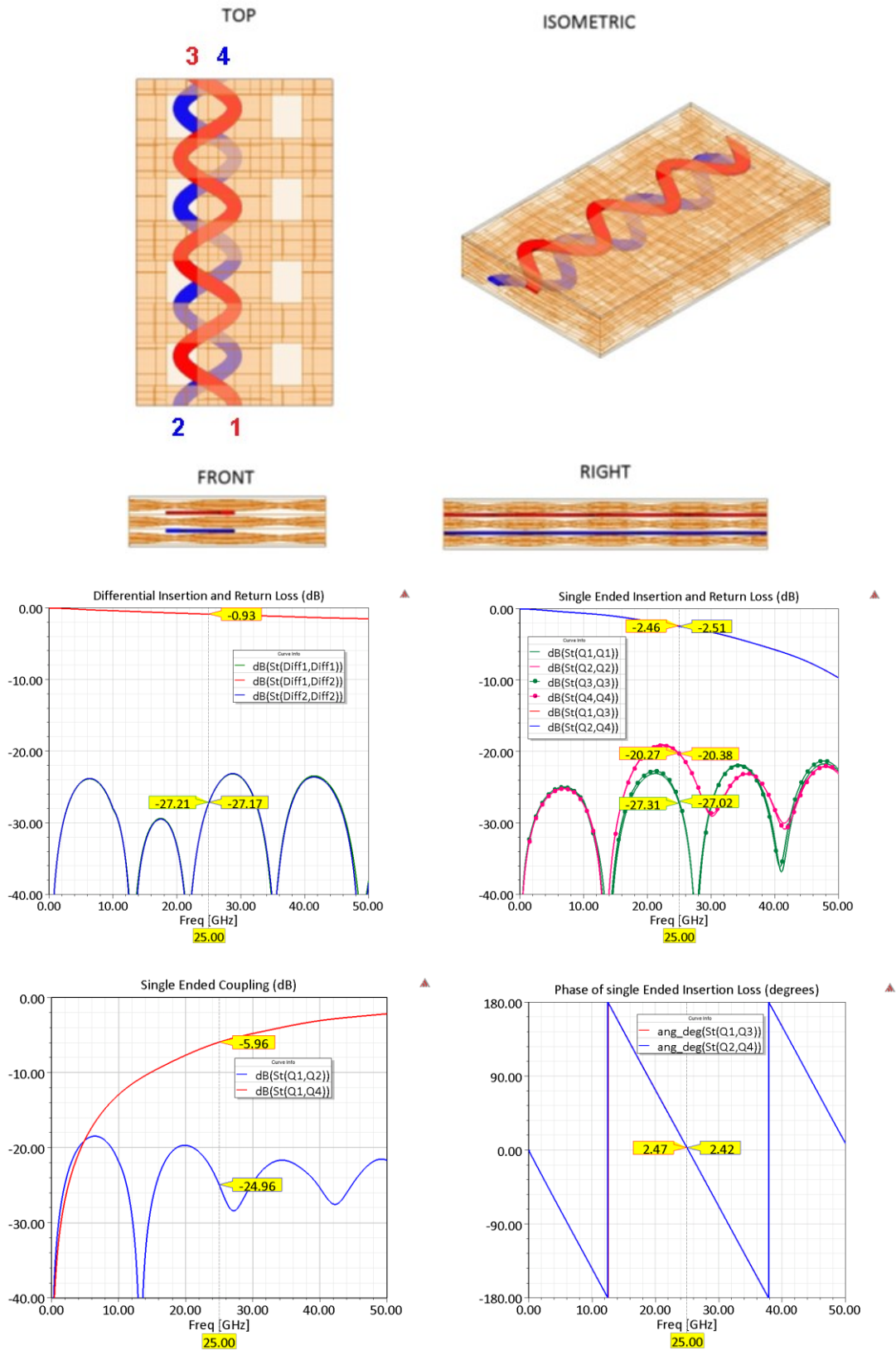
Figure 4: Non-uniform trace geometry on a 200 mils long substrate

3. Effect of skew on the Differential Insertion Loss

The development in reference [11] is extended in this work to include coupling and cascaded transmission line sections.
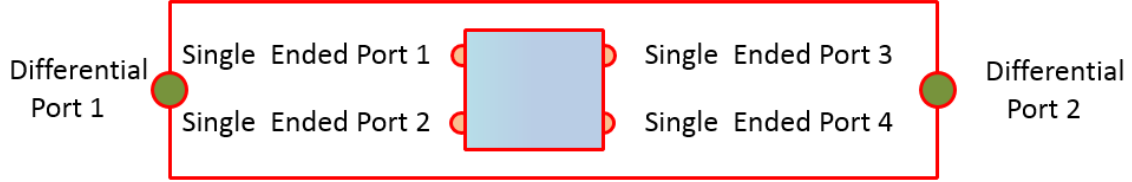

Figure 5: Illustration of a 4 port network and the Port numbering convention used

For a four port network, the normalized incident waves a and reflected waves b are related by the normalized scattering matrix $[S]$ as

$$\begin{bmatrix} b_1 \\ b_2 \\ b_3 \\ b_4 \end{bmatrix} = \begin{bmatrix} S_{11} & S_{12} & S_{13} & S_{14} \\ S_{21} & S_{22} & S_{23} & S_{24} \\ S_{31} & S_{32} & S_{33} & S_{34} \\ S_{41} & S_{42} & S_{43} & S_{44} \end{bmatrix} \begin{bmatrix} a_1 \\ a_2 \\ a_3 \\ a_4 \end{bmatrix} = [S] \begin{bmatrix} a_1 \\ a_2 \\ a_3 \\ a_4 \end{bmatrix} \tag{2}$$

S-parameter matrices are not well suited for cascading and therefore chain matrices or T-parameter matrices become necessary. A new T-matrix definition developed in [13] is utilized here. For a 4 port network, it has the form

$$\begin{bmatrix} b_1 \\ a_1 \\ b_2 \\ a_2 \end{bmatrix} = \begin{bmatrix} T_{11} & T_{12} & T_{13} & T_{14} \\ T_{21} & T_{22} & T_{23} & T_{24} \\ T_{31} & T_{32} & T_{33} & T_{34} \\ T_{41} & T_{42} & T_{43} & T_{44} \end{bmatrix} \begin{bmatrix} a_3 \\ b_3 \\ a_4 \\ b_4 \end{bmatrix} = [T] \begin{bmatrix} a_3 \\ b_3 \\ a_4 \\ b_4 \end{bmatrix} \tag{3}$$

For a cascade connection of 2 four port networks A and B, the s-parameters are obtained from the equation

$$[S]_{A\_cascade\_B} = Convert\_T\_to\_S\ [T]_A [T]_B \tag{4}$$

Equations for the transformation of S to T parameters and vice versa can be found in reference [13].

The differential Insertion loss can then be obtained using

$$S_{DD12} = 0.5 \ (S_{13} + S_{24} - S_{14} - S_{23}) \tag{5}$$

To model skew alone, we will assume a perfectly matched, reciprocal and uncoupled 4 port network comprising two 2-port networks that have a phase difference $\Delta\theta$ and an identical attenuation A.

A skew value of Δt between the single ended ports 1-3 and 2-4 will translate into a phase difference of $\Delta\theta$ which are related by

$$\Delta\theta = 2\pi f \Delta t \tag{6}$$

Where f is the frequency

Figure 6: Symbolic representation of an uncoupled diff pair with skew

In this case:

$$S_{11} = S_{22} = S_{33} = S_{44} = 0$$

$$S_{12} = S_{21} = S_{34} = S_{43} = 0$$

$$S_{14} = S_{23} = S_{41} = S_{32} = 0$$

$$S_{13} = S_{31} = Ae^{j\left(\theta + \frac{\Delta\theta}{2}\right)}$$
$$S_{24} = S_{42} = Ae^{j\left(\theta - \frac{\Delta\theta}{2}\right)}$$

Its T parameter matrix is

$$[T_{skewed}] = \begin{bmatrix} Ae^{j\left(\theta+\frac{\Delta\theta}{2}\right)} & 0 & 0 & 0 \\ 0 & Ae^{j\left(\theta+\frac{\Delta\theta}{2}\right)} & 0 & 0 \\ 0 & 0 & e^{-j\left(\theta+\frac{\Delta\theta}{2}\right)}/A & 0 \\ 0 & 0 & 0 & e^{-j\left(\theta+\frac{\Delta\theta}{2}\right)}/A \end{bmatrix} \quad (7)$$

Next, the case of a coupled differential pair is considered.

Figure 7: Symbolic representation of a coupled diff pair without skew

In this case, let

$$S_{11} = S_{22} = S_{33} = S_{44} = R$$

$$S_{12} = S_{21} = S_{34} = S_{43} = N$$

$$S_{14} = S_{23} = S_{41} = S_{32} = F$$

$$S_{13} = S_{24} = S_{31} = S_{42} = I$$

$$[T_{coupled}] =$$

$$\frac{1}{(I^2-F^2)}\begin{bmatrix} I\,(I^2-F^2-R^2-N^2)+2RFN & F\,(I^2-F^2+R^2+N^2)-2NRI & RI-NF & NI-RF \\ F\,(I^2-F^2+R^2+N^2)-2NRI & I\,(I^2-F^2-R^2-N^2)+2RFN & NI-RF & RI-NF \\ NF-RI & RF-NI & I & -F \\ RF-NI & NF-RI & -F & I \end{bmatrix}$$

$$(8)$$

Using the geometries in Figures 6 and 7, one can model arbitrary values of skew and coupling.

For example, for a coupled network without skew, its s-parameters can be obtained from

$$[S] = Convert\_T\_to\_S\left\{[T]_{coupled}\right\} \tag{9}$$

The differential insertion loss in this case reduces to

$$|S_{DD12}| = |I - F| \tag{10}$$

For a skewed network without coupling, the s-parameters can be obtained from

$$[S] = Convert\_T\_to\_S\left\{[T]_{skewed}\right\} \tag{11}$$

The differential insertion loss in this case reduces to

$$|S_{DD12}| = A \left|Cos\left(\frac{\Delta\theta}{2}\right)\right| \tag{12}$$

Which can be seen to be zero for values of $\left(\frac{\Delta\theta}{2}\right)$ that are integral multiples of $\left(\frac{\pi}{2}\right)$. This will occur at all frequencies where

$$f = \left(\frac{2n-1}{2\Delta t}\right), n \geq 1 \tag{13}$$

For a skewed network with coupling, the s-parameters can be obtained from

$$[S] = Convert\_T\_to\_S\left\{[T]_{skewed}[T]_{coupled}\right\} \tag{14}$$

The differential insertion loss in this case reduces to

$$|S_{DD12}| = A \left|(I - F) Cos\left(\frac{\Delta\theta}{2}\right)\right| \tag{15}$$

It is interesting to see that the skew dependent zero in the differential insertion loss is still present although the slope in its neighborhood is affected by F. This implies that strong coupling alone will not eliminate the null in differential insertion loss arising from skew.

Let us now assume that there are two cascaded networks with skew. We will also assume that they are identical. The s-parameters can be obtained from the following equation.

$$[S] = Convert\_T\_to\_S\left\{[T]_{skewed}[T]_{coupled}[T]_{skewed}[T]_{coupled}\right\} \qquad (16)$$

Equation (16) leads to a large number of algebraic terms. If we neglect higher powers of the s-parameters one obtains

$$|S_{DD12}| \approx A^2 \left|(I - F)\left[I\, Cos(\Delta\theta) - F\right]\right| \qquad (17)$$

It is interesting to see from Equation 17 that the FEXT term F can help in eliminating or displacing the null in the differential insertion loss. It is also clear that $|F|\, must\, be\, > 0$, otherwise Equation 17 will reduce to Equation 15. Mathematically, Equation 17 can still become zero for certain combinations of values of I, F and skew. However, it is not a direct function of skew like Equation 15. It turns out that two or more sections of tightly coupled lines are needed to benefit from this advantage. Further, they need to be placed at locations that is determined numerically. Fortunately, the sensitivity is not very high providing flexibility in adapting to many real situations.

4. Differential Interconnects with large FEXT

From section 3, it can be seen that coupled interconnects that have large values of FEXT are needed. While many such geometries can be constructed, the following two are used in the illustration.

4.1 Vias

It is known that long vias such as those used in backplane connectors have substantial amounts of forward coupling. In the illustration, a differential via in a 20 layer backplane is considered. The via drill diameter is 17 mils and the pad diameter is 30 mils. The spacing between P and N vias is 60 mils, and their spacing to neighboring ground vias is 40 mils. Computed s-parameters are shown in Figure 8. It can be seen that considerable amount of forward coupling is obtained. From the values of single ended and differential insertion loss, FEXT can be seen to help reduce the differential insertion loss.
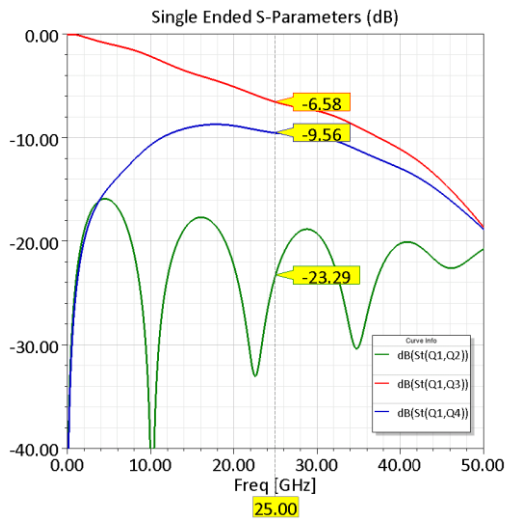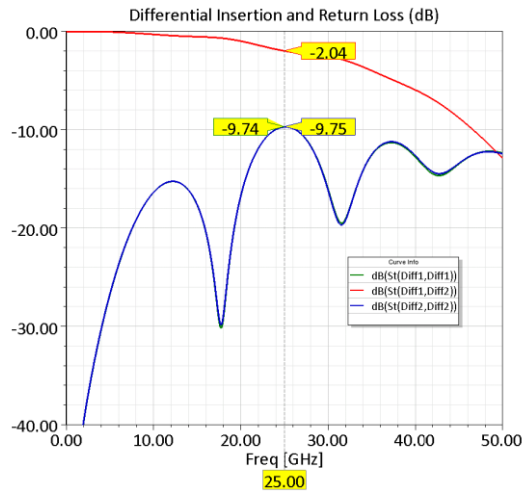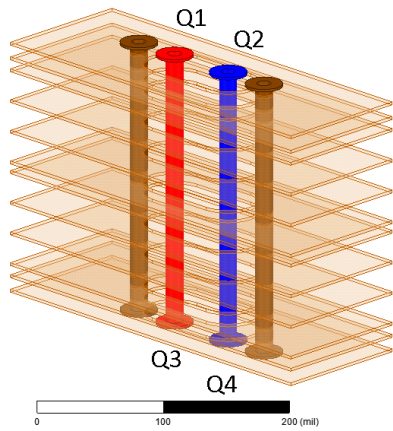
Figure 8: Via geometry and computed s-parameters

4.2 Non-Uniform traces

The non-uniform trace configuration introduced earlier can be designed to yield very large values of FEXT. This structure essentially works like a "coupler" [14]. To understand wave propagation we first consider the case of a straight broad-edge coupled trace in a homogeneous substrate (Figure 10). In this illustration, W = 4 mils, S = 25 mils, T = 0.6 mils, D1= D3 = 4 mils, D2= 3 mils, ε_r= 3.5, tan δ = 0.008, trace length = 500 mils. The total electric field distribution on a plane in between the two traces is also shown for both modes of excitation. At 25 GHz, the line is 2 guide wavelengths long and 4 maxima in the electric field can be seen for both modes of excitation. In this case, it is obvious that the velocities of propagation of both modes, odd (or differential) and even (or common) are the same.
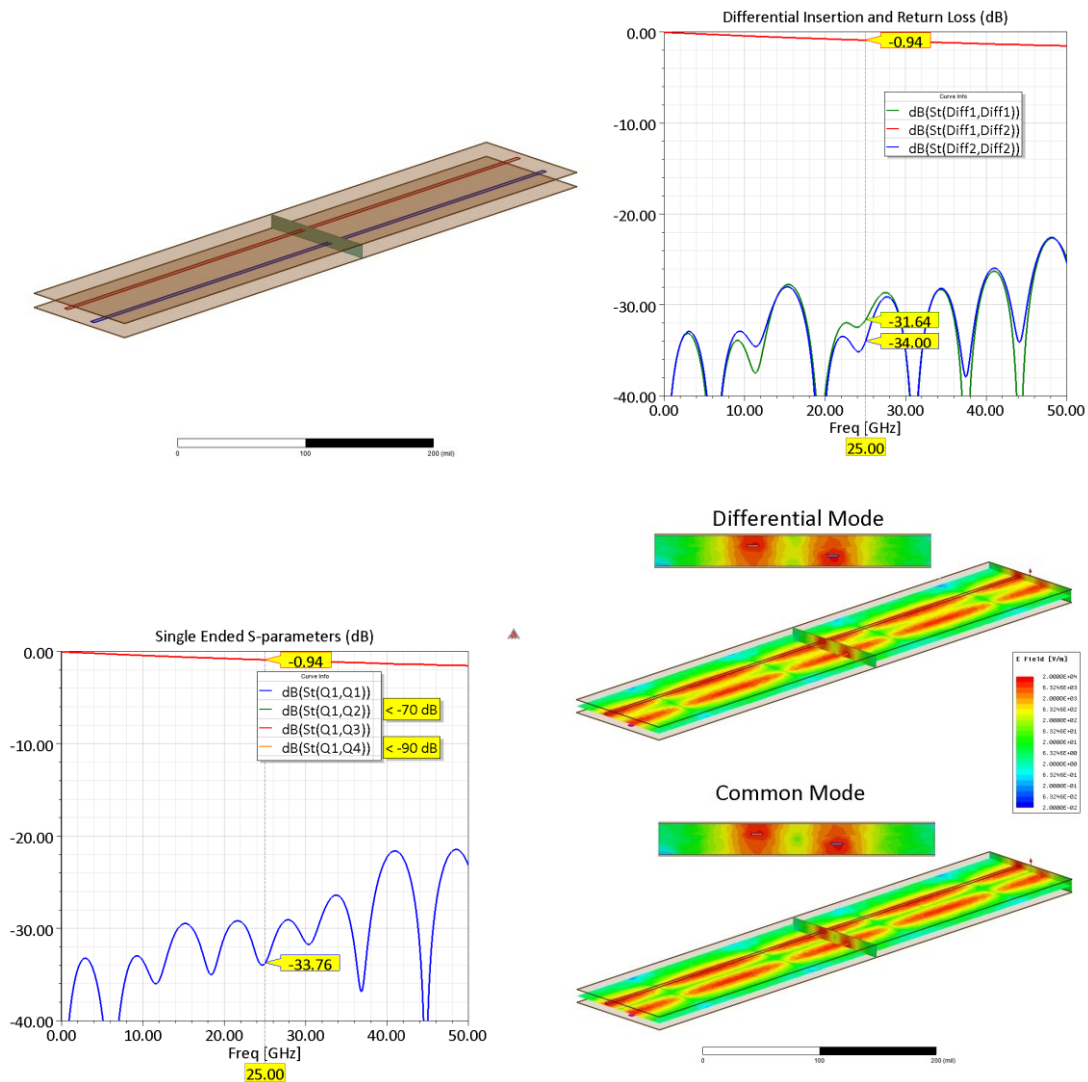
Figure 10: Straight broad-edge trace characteristics

The non-uniform pair in the same stackup is constructed using the equation

$$x(t) = t, \ y(t) = \left(\frac{S+W}{2}\right) Cos\left(\frac{\pi t}{25}\right), 0 \leq t \leq 500 \ mils \tag{18}$$

Field distribution plots in Figure 11 clearly show a difference in propagation velocities of the odd and the even modes. As a result, the structure behaves as a coupler with maximum coupling occuring at frequency that is inversely proportional to the difference in velocities.
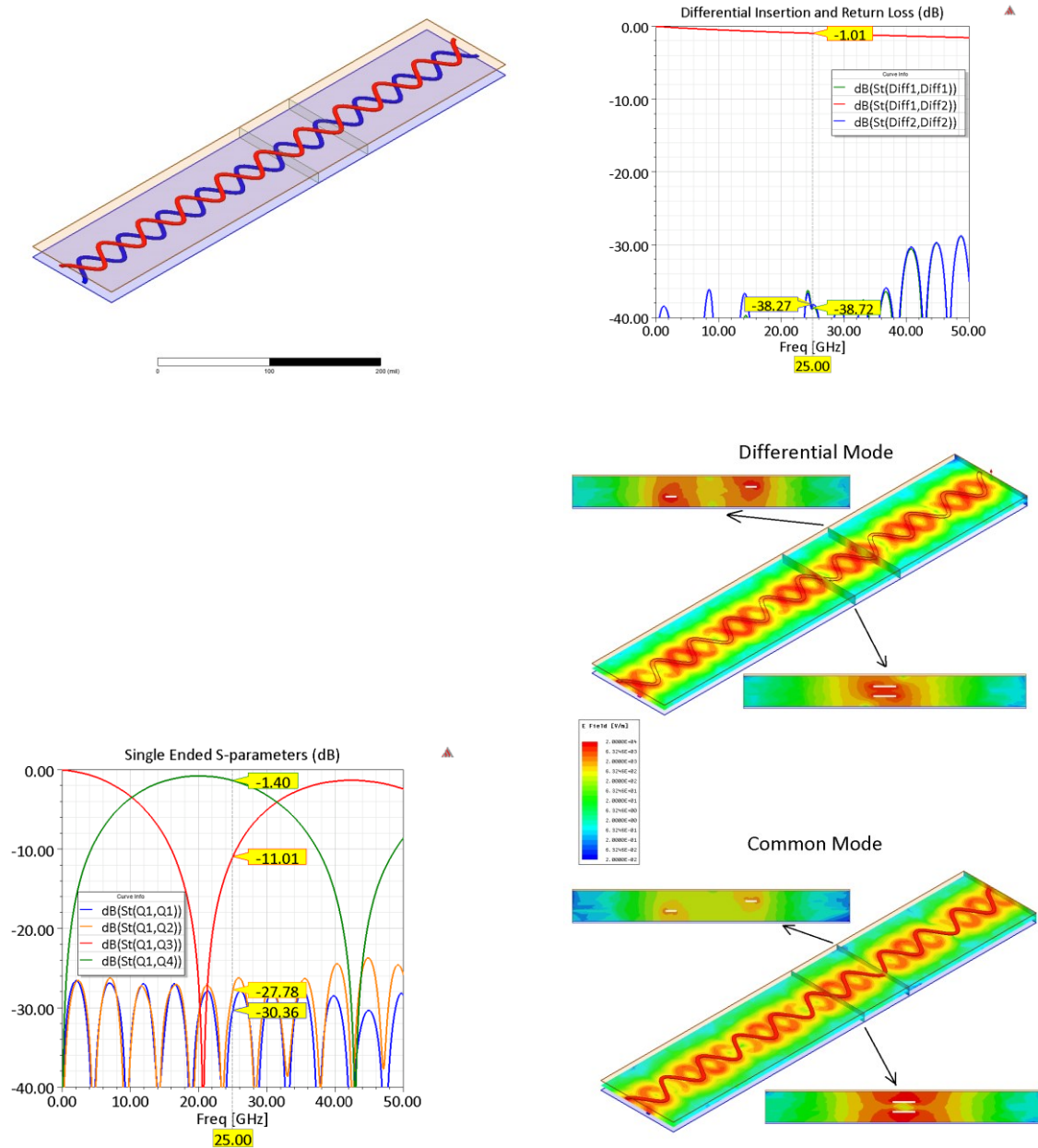

Figure 11: Non-uniform trace characteristics

5. Numerical illustration and Conclusion

The following example is used to illustrate the benefit obtainable by inserting tightly coupled sections into an interconnect path that can be affected by fiber weave skew. The modeling method of reference [10] is used. This consists of using short sections of transmission lines with an ideal delay element to represent fiber weave skew.

The reference example (Figure 12, Case A) is a 9 inch long single ended stripline (W = 4.35 mils, T = 0.6 mils, D1= D3 = 4.5 mils, ε_r= 3.5, tan δ = 0.008. It is implemented as a cascade connection of 9 one-inch long sections. The skewed case B is simulated by the inclusion of a 3.47 pS of delay in one the lines as shown. The number is chosen to result in a null at 16 GHz.

Computed results are shown in Figure 13. The well-known effect of skew which produces a null at 16 GHz (Equation 13) is apparent. A plot of the differential to common mode transfer s-parameter S_{CD12}, is also shown. It can be seen that common mode conversion will be substantial where the differential mode has a null.

Cases C and D in Figure 14 illustrate use of tightly coupled sections. Their number and location was determined by trial and error. Computed differential insertion loss is shown in Figure 15 where all four results are super-imposed. It can be seen that in both cases C and D the null at 16 GHz caused by skew is no longer present. With case D, the attenuation at 16 GHz is only worse than that of case A by less than 3 dB. The differential to common mode conversion s-parameter results in Figure 16 also show an improvement.

To get a better understanding of how this is achieved, single ended s-parameters of both cases are plotted in Figures 17-18. In the case of the via, it is clear that S_{24} is attenuated substantially at 16 GHz as compared to S_{13}, and consequently the creation of a null is averted. Case D is somewhat more complicated. Here the amplitudes of all four components of the differential insertion loss (Equation 5) are approximately the same. It is their phases that prevent a null formation.

Finally, the effect of these interconnects on the eye diagram is illustrated by using them in a 32 Gbps link. The driver transmits a maximum amplitude signal with some pre- and post-emphasis and the receiver uses a 5-tap adaptive DFE. Computed Eye diagrams using Keysoft' ADS and interconnects of cases A, C and D are shown in Figure 19. Eye closure results with Case B and is not shown. It can be seen that the insertion of tightly coupled sections does not have any significant effect on eye opening other than what is expected from the increased attenuation as compared to the reference case A.

The non-uniform geometry of Section 4.1 would be useful in cost, layer count and thickness constrained designs. Flexible PCBs would be one area. Use of tightly coupled elements is beneficial in multi-board interconnects and can prevent accumulation of fiber weave skew. Designing using these elements requires numerical simulation and optimization.
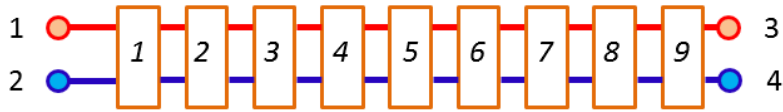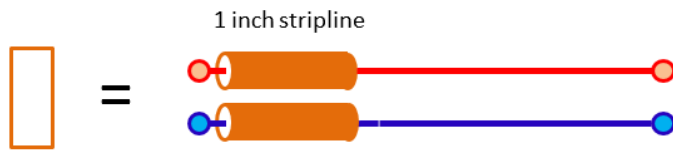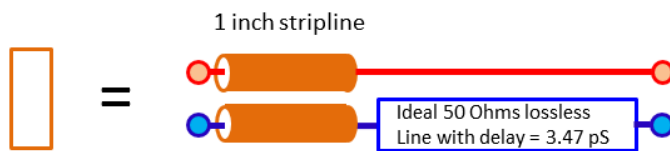
Figure 12: Cascaded transmission line sections used in the illustration.
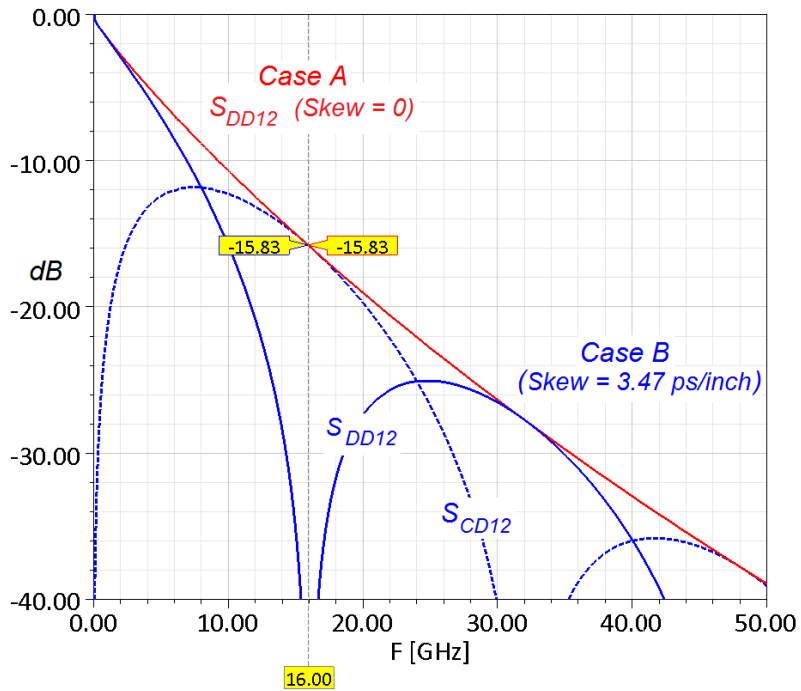
Figure 13: Computed Differential insertion loss of cases A and B
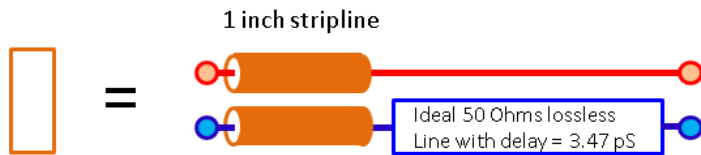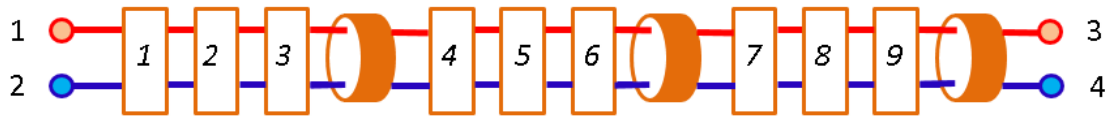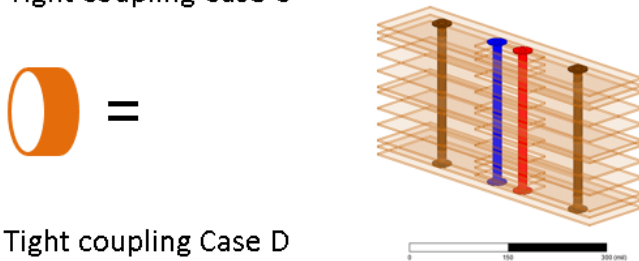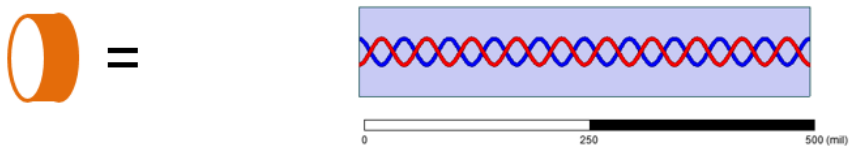
Figure 14: Illustration of cases C and D
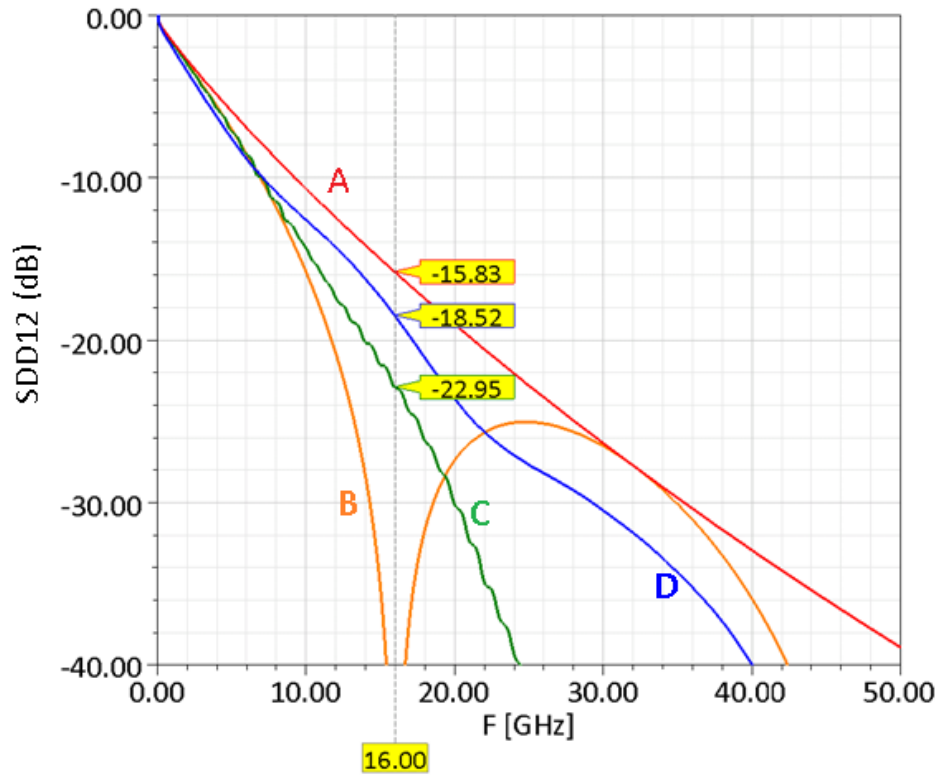
Figure 15: Comparison of Differential Insertion Loss
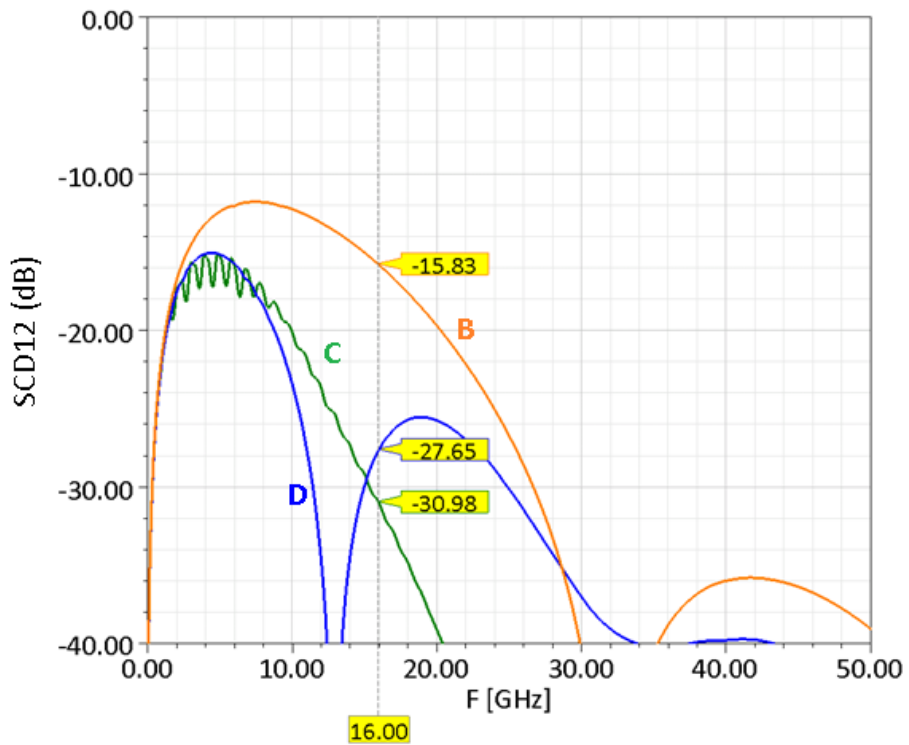
Figure 16: Comparison of Differential to Common mode Insertion Loss
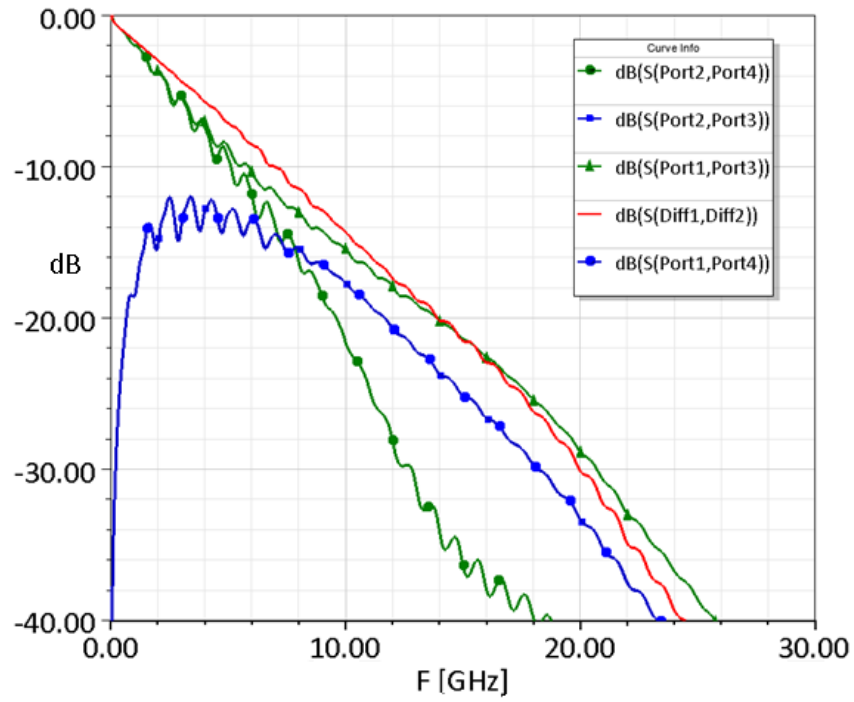
Figure 17: S-parameters of case C
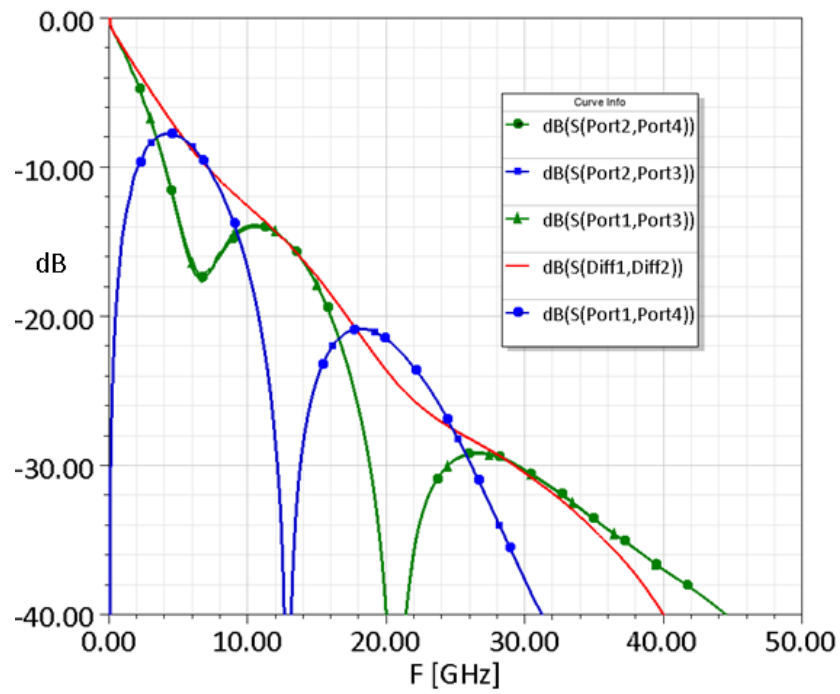

Figure 18: S-parameters of case D
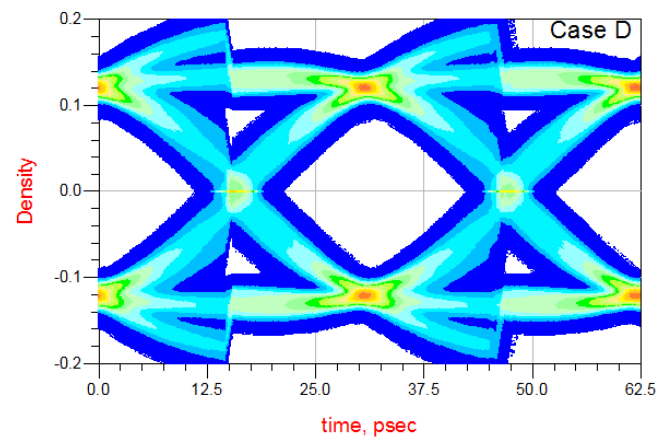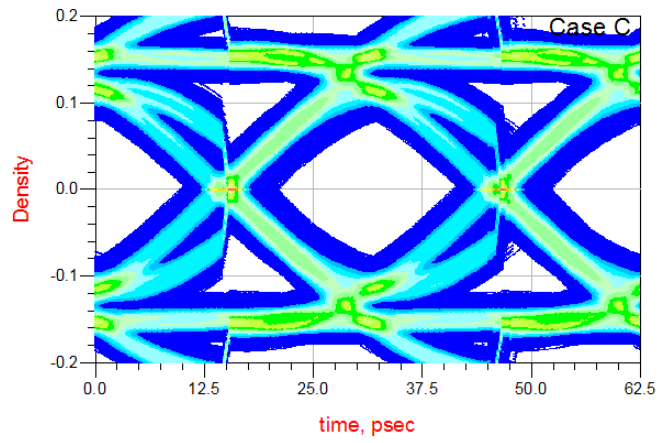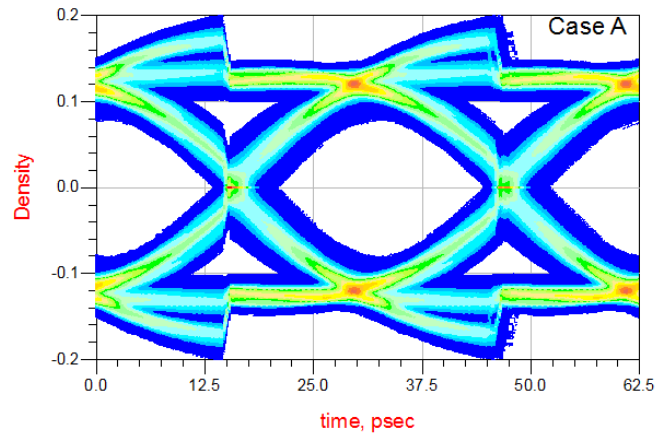
Figure 19: 32 Gbps Eye diagrams of cases A, C and D

References

[1] B. Gore, and R. Mellitz, "An exercise in applying Channel operating margin for 10GBASE-KR Channel Design", Proceedings of the IEEE EMC Symposium, Rayleigh, NC., 2014, pp. 648-653.

[2] Eben Kunz, Jae Young Choi, Vijay Kunda, Laura Kocubinski,Ying Li, Jason Miller, Gustavo Blando, and Istvan Novak, "Sources and Compensation of Skew in Single-Ended and Differential Interconnects, Signal Integrity Journal, April 2017.

[3] Syed Bokhari, "Debugging High speed SERDES issues in multi-board interconnect systems", Proceedings EDICON 2017, Boston.
     (https://www.signalintegrityjournal.com/authors/134-syed-bokhari)

[4] Scott McMorrow, C. Heard, "The Impact of PCB Laminate Weave on the Electrical Performance of Differential Signaling at Multi-Gigabit Data Rates," DesignCon 2005.

[5] J. Loyer, R. Kunze, and Xiaoning Ye, "Fiber Weave Effect: Practical Impact Analysis and Mitigation Strategies", Proceedings of DesignCon 2007, pp. 1-28.

[6] Lambert Simonovich, "Practical Fibre Weave Effect Modeling" , White paper issue2,Lamisim enterprises Inc. Oct 2011.
     (www.magazines007.com/pdf/PFWEM.pdf)

[7] Yuriy Shlepnev and Chudy Nwachukwu, "Modelling Skew and Jitter induced by fibre weave effect in PCB dielectrics", Proceedings of 2014 IEEE International Symposium on Electromagnetic Compatibility, Raleigh, North Carolina, August 7, 2014.

[8] Tomoyuki Akahoshi, Teng-Kai Chen, Taiga Fukumori , Yasuo Hidaka, Kenichi Kawai, Michael Lee, Mark Lionbarger, Daisuke Mizutani ,Yasushi Mizutani Hideaki Nagaoka , Tetsuro Yamada, Takuji Yamamoto, "Mitigation of Fiber-Weave Effects by Broadside-Coupled Differential Striplines", DesignCon 2015.

[9] E. Bogatin, B. Hargin, V.S.Sai. D. DeGroot, A. Koul, S. Baek, and M. Sapozhnikov, "New Characterization Techniques for Glass Weave Skew (Part 2)" , Proceedings DesignCON 2017.

[10] Amendra Koul, Kartheek Nalla, David Nozadze, Mike Sapozhnikov, Yaochao Yang, "Fiber weave effect: Modeling, measurements, challenges and its impact on differential insertion loss for weak and strong-coupled differential transmission lines", DesignCon 2018.

[11] S. Farrahi, V. Kunda, Y. Li, X. Zhang, G. Blando, and I. Novak, "Does skew really degrade SERDES performance?", Proceedings DesignCON 2015, pp.1-19.

[12] Syed Bokhari, "Non –uniform transmission line for reducing crosstalk from an aggressor line", US Patent 7397320, July 8, 2008.

[13] James Frei, Xiao-Ding Cai, and Stephen Muller, "Multiport S-Parameter and T-Parameter conversion with symmetry extension", IEEE Transactions on Microwave Theory and Techniques, vol. 56, No.11, November 2008, pp.2493-2504.

[14] Dan Piscotty, Julian Ferry and Richard A. Elco, "The Samtec Golden Standard: A Reference Structure for Electrical Simulation and Measurement: Parts I and II, 2005, www.samtec.com.